Fuel 324 (2022) 124753

Contents lists available at ScienceDirect

Fuel

journal homepage: www.elsevier.com/locate/fuel

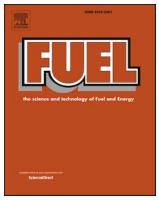

Full Length Article

Carbon-based monoliths with improved thermal and mechanical properties for methane storage

S. Reljic, C. Cuadrado-Collados, J. Farrando-Perez, E.O. Jardim, M. Martinez-Escandell, J. Silvestre-Albero *

Laboratorio de Materiales Avanzados, Departamento de Química Inorgánica-Instituto Universitario de Materiales, Universidad de Alicante, Spain

ARTICLE INFO

Keywords:
Activated carbon
Carbon monoliths
Methane storage
Graphene
Graphite

ABSTRACT

A series of activated carbon materials have been prepared from petroleum residue using KOH as activating agent. The gravimetric adsorption capacity for methane of the synthesized samples increases with the activation degree, albeit at a lower packing density of the carbon material. These results anticipate an optimum pitch/KOH ratio (1:3) to achieve an upper limit in the volumetric storage capacity. Activated carbon powders have been conformed into monoliths using a small amount of a binder (5 wt%), either carboxymethyl cellulose or polyvinyl alcohol, with proper mechanical properties. Incorporation of graphite or graphene in the initial formulation does not alter and/or modify significantly the textural properties of the original activated carbon. However, once conformed into monoliths, the presence of graphite or graphene allows to improve i) the packing density of the monoliths (up to 0.52 g/cm^3), ii) their mechanical properties (compressive strength ≈ 12.3 MPa) and iii) their thermal conductivity (up to 0.49 W/mK) without compromising the methane storage capacity (ca. 100 V/V).

1. Introduction

Porous materials (activated carbons and metal–organic frameworks, among others) have been widely applied in the literature for a number of cutting edge processes, from gas adsorption/separation, [1–5] sensors, [6,7] drug delivery, [8–11] etc. The excellent performance of these materials is based on the presence of a widely developed porous structure and, in some cases, a perfectly tailored surface chemistry. However, bridging the gap from fundamental studies to a potential industrial application of these materials is not straightforward and, indeed, some limitations are still on the ground and require further investigation. One of these limitations concern the densification of these powder samples into pellets, monoliths or any other shape. The conformation of these porous networks is mandatory i) to minimize pressure drops in gas and liquid-phase adsorption processes, ii) to facilitate the manipulation of the material (charging and discharging), iii) to densify the samples (to reduce the interparticle space and the macroporosity) and iv) to minimize environmental and health issues due to particulates [12,13]. For instance, the conforming step is extremely important for gas adsorption/storage applications due to the necessity to trap a large amount of a target molecule (e.g., CH_4, CO_2 or H_2 storage in porous solids) in a minimum volume (for instance, in automotive applications).

The conforming step is traditionally performed through the incorporation of a binding agent in the final formulation and application of a mechanical stress [14,15]. However, novel approaches based on soft, hard, dual or non-templated methods have been widely reported in the literature [16–22]. As expected, these approaches are highly sensitive to the type of material to be conformed, the precursor used (specifically in the case of carbon materials) and the requested final properties. Although densification is a crucial step to bridge the gap towards industrial application of porous solids, in some cases, additional properties are required. For instance, electrical conductivity is required when these materials have to be applied in supercapacitors or batteries [23,24]. In a similar fashion, thermal conductivity is needed for high-pressure storage devices [25,26]. In fact, heat generated during adsorption (exothermic process) has to be immediately released from the reactor bed to avoid thermal spikes during the adsorption step that will limit the adsorption performance of the adsorbent. Contrariwise, heat has to be supplied to the adsorbent to favor the desorption of the retained molecules. Unfortunately, traditional adsorbents such as activated carbons, zeolites or metal–organic frameworks exhibit poor thermal properties, with the subsequent limitations for gas storage processes [27,28]. Thermal management can be performed either through the incorporation of heat exchanging devices into the storage vessel (e.g., honeycomb heat

* Corresponding author.
E-mail address: joaquin.silvestre@ua.es (J. Silvestre-Albero).

https://doi.org/10.1016/j.fuel.2022.124753
Received 21 March 2022; Received in revised form 5 May 2022; Accepted 2 June 2022
Available online 14 June 2022

exchanging system) or through the modification of the adsorbent to enhance the heat conductivity [29–35]. Among the different alternatives to improve thermal properties, the incorporation of carbon-based additives with an enhanced electrical and/or thermal performance, such as graphene or graphite derivatives constitutes a promising approach. Zhang et al. synthesized graphene/carbon aerogels from polyimide with improved electrical properties for supercapacitors [31]. Menard et al. made an activated carbon in situ elaborated within a consolidated expanded natural graphite with improved thermal properties [32]. A significant improvement in the thermal conductivity of anthracite-based activated carbons was described by Kuwagati et al. after incorporation of graphite in the final formulation of the monolith [33]. Despite these improvements, the synthesized monoliths require additionally proper mechanical properties to avoid particulates due to attrition processes.

Despite the relevance of these topics for a real application, the number of studies reported in the literature concerning the conformation of porous materials (mainly carbon materials) into monoliths with enhanced mechanical and thermal properties is rather limited. Based on these premises, the main goal of the present manuscript is the synthesis and modification of petroleum-based pitches, characterized by a good adsorption performance, through the incorporation of high thermal conductivity additives (e.g., graphene or graphite) and their subsequent application in methane storage at medium pressures (4 MPa). The synthesized carbon-based monoliths have been evaluated in terms of adsorption capacity (gravimetric vs volumetric), mechanical and thermal properties. The final objective is to incorporate a minimum amount of additive to improve mechanical and thermal properties without compromising the excellent adsorption performance of the original petroleum-pitch activated carbons.

2. Materials and methods

2.1. Preparation of the petroleum-pitch activated carbons

Activated carbon materials have been prepared from petroleum pitch as carbon precursors. In an initial step, the original petroleum pitch (PP) was pyrolyzed at 733 K under a nitrogen atmosphere (1 MPa) for 90 min (pyrolysis yield 52 %). The pyrolyzed PP sample was grounded in a ball mill until a fine powder was achieved (500 μm particle size). In a subsequent step, the mesophase pitch was mixed with KOH as a chemical activating agent in a ball mill until a homogenous mixture is obtained. Five different pitch/KOH ratios were evaluated, from 1:1 up to 1:5. The carbon samples were activated at 973 K for 2 h using a nitrogen flow of 100 ml/min. Last but not least, the synthesized carbons were washed with HCl (37 %) and distilled water until neutral pH, and finally dried at 348 K overnight. The activation yield range from 61 % for the PPAC1:1 sample down to 49 % for the PPAC1:5 sample. Samples were labeled PPAC1:x (x = 1–5).

2.2. Preparation of graphite/graphene-modified activated carbons

Once the proper activation conditions were identified (pitch/KOH ratio 1:3), three additional samples were prepared using either graphite or graphene as additives. Synthetic graphite powder (1–2 μm) was obtained from Sigma-Aldrich and graphene was purchased from Avanzare ltd. (Spain). Either graphite or graphene were mixed with the original petroleum pitch (after pyrolysis) and grounded in the ball mill for 30 min at 300 rpm. The mixture was stabilized through a thermal treatment in a horizontal oven at 673 K for 1 h under a nitrogen atmosphere (100 ml/min). Afterwards, the fine powder was mixed with KOH (pitch + graphite/graphene:KOH ratio of 1:3) in a ball mill for 30 min and activated in a horizontal oven using the same conditions described above. Samples were labeled PPAC1:x_yGI, for graphite or _yGE, for graphene (y = amount of additive incorporated).

2.3. Preparation of the monoliths

For the preparation of the monoliths, two different binders were evaluated: carboxymethyl cellulose (CMC) and polyvinyl alcohol (PVA). In the specific case of CMC, the corresponding amount of binder was dissolved in water to make a gel. The activated carbon powder (300–500 mg) was added to the gel to make a slurry. The mixture was conformed into disk-shaped monoliths under different loads, i.e. 1, 3 and 5 tons (corresponding pressures 74, 222 and 370 MPa, respectively, after considering the cross-sectional area of the monolith (ca. 1.32 cm^2)). The synthesized monoliths were heat treated in an oven at 348 K to evaporate the remaining water. In the specific case of PVA, the corresponding amount of binder was slowly mixed with cold water under stirring. The mixture was subsequently heated at 363 K for 30 min until complete dissolution. The cooled solution was admixed to the carbon powder to form a slurry. The wet mixture was conformed into a disk-shaped monolith at 1 ton. A stain-steel mold with i.d. 1.3 cm was used for all samples. To end up, the monoliths were heat treated in an oven at 348 K to remove all the remaining water.

2.4. Sample characterization

The textural properties of the synthesized samples were evaluated using gas adsorption measurements at cryogenic temperatures (N_2 at 77 K). Before the adsorption measurements, samples were outgassed under ultra-high vacuum (UHV) conditions at 523 K for 4 h. Nitrogen adsorption measurements were performed in a home-built manometric system. Thermal conductivity of the synthesized monoliths was evaluated using a thermal analyzer C-Therm TCi from Mathis Instruments ltd. based on the modified transient plane source (MTPS) principle. The compressive strength measurements were performed in a 5 KN Instron Universal testing machine model 4411, using parallel plates. The tests were performed at a 0.1 mm/min deformation rate using cylindrical samples of 1.3 cm diameter and 0.5 cm height. Compressive modulus was calculated form the slope of the stress/strain curve in the linear region. Compressive strength was determined as the maximum value of stress in the stress/strain curve before the failure of the sample.

2.5. High-pressure methane adsorption measurements

High-pressure excess methane adsorption measurements were performed at 298 K in a home-built manometric equipment [36]. Before the adsorption measurement, the samples were outgassed in-situ at 523 K for 4 h. In the specific case of the monoliths, a specially designed sample cell was used to allow measuring the adsorption performance of the complete monoliths.

3. Results and discussion

3.1. Activated carbon-based materials in powder form

3.1.1. Effect of the amount of activating agent

One of the main parameters defining the development of the porosity in carbon materials, and indirectly, their adsorption performance is the nature and the amount of activating agent used. It has been widely accepted in the literature that KOH as activating agent gives rise to carbon materials with a widely developed porous structure, preferentially in the narrow microporous range [37–40]. Fig. 1a shows the nitrogen adsorption/desorption isotherms for PPAC samples prepared with a pitch/KOH ratio ranging from 1:1 to 1:5. As it can be appreciated, all synthesized samples are microporous in nature, the amount of nitrogen adsorbed increasing with the activation degree. While samples with a low pitch/KOH ratio (e.g., 1:1) exhibits a narrow pore size distribution (a narrow knee can be appreciated in the nitrogen isotherm), samples with 1:5 ratio exhibit a broad knee due to the presence of narrow and wide micropores. The apparent BET surface area ranges

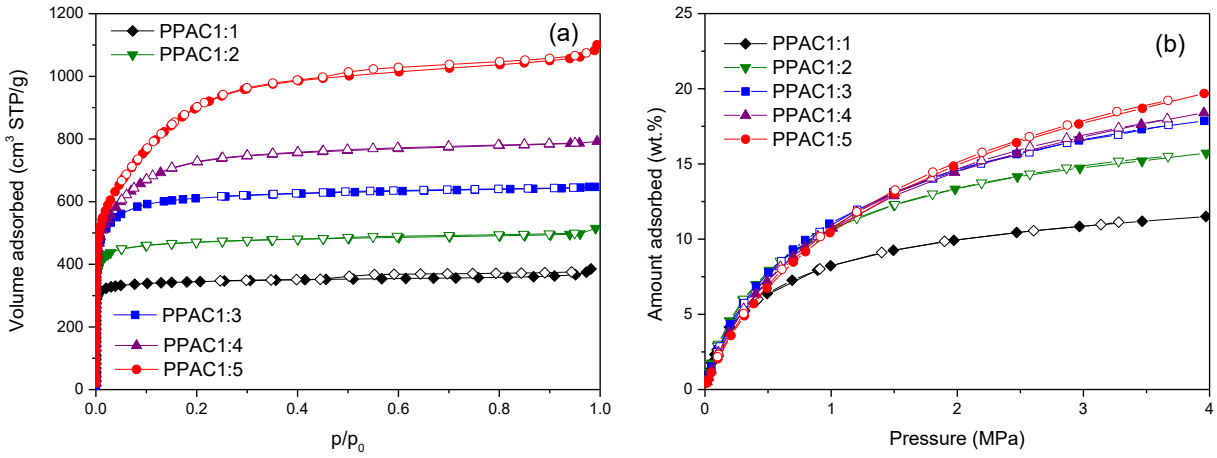

Fig. 1. (a) Nitrogen adsorption/desorption isotherms at 77 K for the PPAC samples prepared using KOH as activating agent (pitch/KOH ratio from 1:1 up to 1:5); (b) Excess methane adsorbed at 298 K and up to 4.0 MPa for the synthesized samples.

from ca. 1400 m^2/g for sample 1:1, up to 3300 m^2/g for highly activated pitches (see Table S1).

The preferential presence of narrow microporosity in the different KOH activated samples is confirmed in Figure S1. The pore size distribution (PSD) obtained after application of the QSDFT model reflects the presence of a majority of pores below 1 nm, with some contribution in the 1–2 nm range for highly activated samples, and even some mesoporosity, although scarce, above 3 nm for sample PPAC1:5.

Activated carbon materials with a highly developed porous structure are promising platforms for gas adsorption/storage processes [39,40]. In this sense, Fig. 1b shows the methane adsorption performance (excess amount adsorbed) for the synthesized samples up to 4.0 MPa. As expected, the amount of methane adsorbed increases with the activation degree, the effect of the activation being more significant in the low activation range. The excess gravimetric storage capacity obtained ranges from 11.5 wt%, for sample PPAC1:1, up to 20.6 wt%, for sample PPAC1:5, in both cases at 4.0 MPa and 298 K (Table 1). These values in gravimetric basis are among the best described in the literature for carbon materials [41]. Despite the excellent adsorption values obtained in gravimetric basis, it is important to highlight that volumetric storage capacity is more relevant for a subsequent technological application of porous materials due to necessity to adsorb a maximum amount of the target molecule in a minimum volume (or restricted space). However, the conversion from gravimetric to volumetric is not straightforward since the knowledge of the real density of the sample is needed. A closer look to the literature shows that this is a controversial issue since calculations can be performed using either i) packing density of the powder material (with or without binder) under pressure, or ii) packing density of the conformed material after releasing the pressure (sometimes a fragile monolith is obtained when a binder is not used, with the associated uncertainty in measuring the monolith dimensions) or iii) even the crystallographic density of a theoretical single crystal (very typical in the specific case of crystalline materials such as MOFs) [42]. Among these possibilities, the most realistic approach, and the one used in this manuscript, is the second one. This approach implies a direct evaluation of the volume occupied by the compacted powder in a monolithic shape after releasing the pressure, provided that the mechanical properties of the synthesized monolith are appropriate. Table 1 shows the evaluation of the packing density for the different samples evaluated.

Table 1
Gravimetric and volumetric excess methane adsorption capacity for the different PPAC samples. Packing density (g/cm^3) of the powder samples without binder after a conforming step at 74 MPa and activation yield are also included.

Sample	CH_4adsorbed (wt.%) 4.0 MPa	Packing density (g/cm^3)	Activation Yield (%)	CH_4 Adsorbed (V/V)
PPAC1:1	11.5	0.47	63	76
PPAC1:2	15.7	0.42	60	92
PPAC1:3	17.9	0.38	54	95
PPAC1:4	19.0	0.35	46	93
PPAC1:5	20.6	0.33	41	95

As it can be appreciated, the packing density decreases with the development of porosity from 0.47 g/cm^3 down to 0.33 g/cm^3 (to avoid uncertainty with the fragile monoliths (compacted powder), several repetitions have been performed to get an accurate average value; uncertainty is around 4–5 %). Taking into account these values, the calculated volumetric capacity for the synthesized carbons increases from 76 V/V for sample PPAC1:1 up to a plateau around 95 V/V, for samples PPAC1:3 and above. Apparently, although the activation degree improves the adsorption performance in gravimetric basis, the associated decrease in density minimizes this improvement, thus giving rise to an upper limit in the excess volumetric capacity.

3.1.2. *Incorporation of high thermal conductivity additives*

Taking into account the results describe above, sample PPAC1:3 was selected for the subsequent studies. This sample combines a proper development of porosity, a proper density and, consequently, an optimum in the excess volumetric adsorption capacity. One of the main limitations of activated carbons for gas storage applications is their low thermal conductivity. Overall, the limited conductivity is a severe limitation for the majority of inorganic porous solids with potential application in gas adsorption/storage processes, such as zeolites, activated carbons and metal–organic frameworks (thermal conductivity lower than 0.2–0.3 W/mK) [43–45]. A promising approach to improve the thermal conductivity in carbon materials is based on the preparation of composite materials via the incorporation of a small percentage of a second component with a high thermal conductivity, for instance graphene or graphite. To this end, a series of samples have been prepared using petroleum pitch blended with graphite or graphene, followed by a subsequent chemical activation using KOH (see Experimental Section for further details).

Fig. 2a shows the N_2 adsorption/desorption isotherms for the original PPAC1:3 sample and the same pitch modified with 5–10 wt% graphite or 2.5 wt% graphene. At this point it is important to highlight that the differences in the amount of graphite and graphene incorporated are based on their extremely different tap densities (0.35 g/cm^3 vs 0.022 g/cm^3, respectively).

Nitrogen isotherms clearly reflect that the incorporation of a small amount of additive before the activation step does not modify significantly the porous structure of the final composite, although a

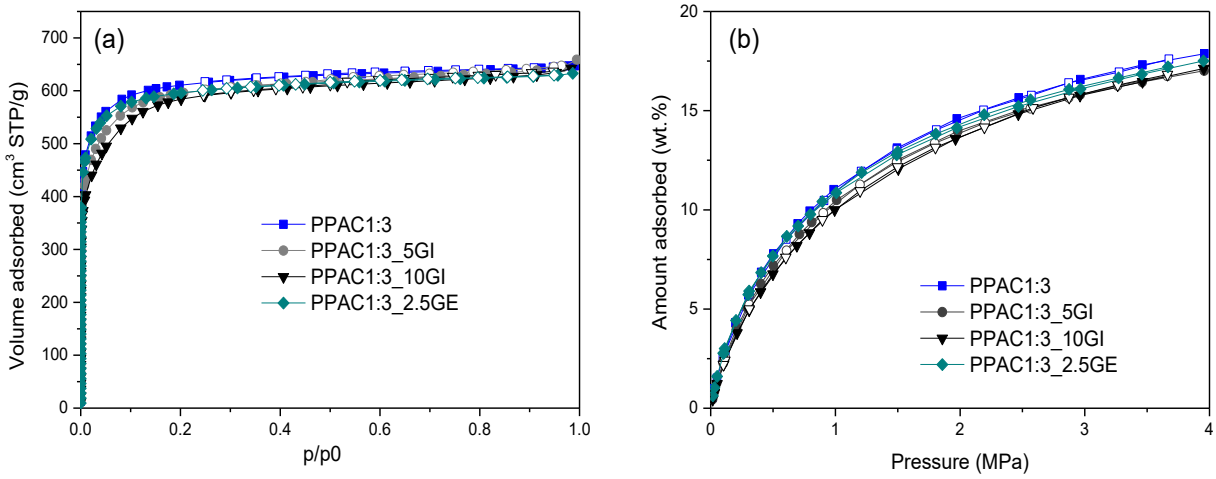

Fig. 2. (a) Nitrogen adsorption/desorption isotherms at 77 K for the PPAC1:3 sample before and after the modification with graphite or graphene; (b) Excess methane adsorbed at 298 K and up to 4.0 MPa.

progressive decrease in the BET surface area can be appreciated. The absence of important changes in the porous network is also reflected in the textural parameters deduced after application of the BET and Dubinin-Radushkevich equations (see Table S2). The presence of a rather similar porous texture is also reflected in the excess methane adsorption performance for the 4 samples evaluated, with a gravimetric uptake values around 17–17.5 wt% (Table 2).

The main difference between the original and the composite samples concerns the packing density. As expected, the incorporation of a second component gives rise to a slight increase in the density from 0.38 g/cm^3 up to 0.43 g/cm^3, after incorporation of 10 wt% graphite, and 0.39 g/cm^3, after incorporation of graphene (2.5 wt%). These changes in the density of the final composite have an effect in the volumetric adsorption capacity, with a slight increase from 95 V/V in the unmodified carbon up to a maximum of 102 V/V for the sample PPAC1:3_10GI. These results reflect that the incorporation of graphene and/or graphite before the activation step give rise to composite materials with a rather similar porosity and adsorption performance but with an improved density due to the higher density of the second component.

3.2. Activated carbon-based materials in monolithic shape

3.2.1. Effect of the conforming conditions (binder amount and nature, conforming pressure, etc.)

As described above in the introduction, one of the main limitations for powder samples is their limited technological applicability due to the associated pressure drops in large reactors. To avoid these drawbacks, powder samples have to be conformed into pellets or monoliths. However, the conforming step is not straightforward due to the necessity to apply high pressures, with the associated structural damage for some kind of materials, and the necessity to incorporate a binder, with the associated partial blocking of the porosity [46]. Although novel routes have been proposed in the literature to synthesize monoliths (for instance the gelation of MOF crystals into monoliths avoiding pressure and the use of a binder), the conventional route using high pressures and binding agents is still the most widely applied [14,15,19,20]. In the specific case of carbon PPAC1:3 we have investigated the role of the binder used (5 wt%), either polyvinyl alcohol - PA or carboxymethyl cellulose - CMC.

Table 2
Gravimetric and volumetric excess methane adsorption capacity for the different PPAC1:3 samples modified with graphite or graphene. Packing density (g/cm^3) of the powder sample without binder after a conforming step at 74 MPa and activation yield are also included.

Sample	CH_4adsorbed (wt.%) 4.0 MPa	Packing density (g/cm^3)	Activation Yield (%)	CH_4 Adsorbed (V/V)
PPAC1:3	17.9	0.38	54	95
PPAC1:3_5GI	17.1	0.40	54	96
PPAC1:3_10GI	17.0	0.43	54	102
PPAC1:3_2.5GE	17.4	0.39	54	95

Figure S2 and Tables S3&S4 clearly anticipates that both monoliths possess a similar porous structure, with an apparent surface area around 2230–2250 m^2/g, a similar density for the monolith (0.41 g/cm^3), and a similar performance for methane storage at 4.0 MPa both gravimetric and volumetric (although slightly larger capacity for the CMC-based monoliths). Compared to the parent powder carbon, PPAC1:3, textural details show that the conforming step does not produce any deterioration of the 3D porous network, in close agreement with the intrinsic strength of carbon materials, except some minimal pore blocking due to the incorporation of the binder. Representative photographs of the monoliths (Fig. 3) confirm that both samples are robust and must possess proper intrinsic mechanical properties (no defects or external deterioration can be appreciated). To further confirm this aspect, the mechanical properties of the synthesized monoliths have been evaluated using conventional compressive stress–strain tests. These analyses are very useful to identify the maximum stress that a monolith can sustain before rupture. Figure S3 shows the stress–strain profiles for the two monoliths evaluated. The compressive modulus obtained from the slope is 57 MPa, for MPPAC_CMC, and 44 MPa, for MPPAC_PVA samples (Table S4). The improved mechanical performance of CMC-based monoliths is also reflected in the compressive strength at the failure point, i.e. 6 MPa for CMC and 4 MPa for PVA-based monoliths. These values are rather similar to those described in the literature for phenolic resin, sucrose and pitch-derived carbon foams [47–49]. With these premises, CMC was selected for the next steps due to the easiness in the preparation of the monoliths (no heat needed compared to PA) and the improved mechanical properties of the monoliths.

Another critical parameter in the preparation of monoliths concerns the total pressure applied during the conforming step since high pressures can be detrimental for the 3D porous network [46]. Figure S4 and Tables S5&S6 compare the adsorption performance of PPAC monoliths prepared with CMC as a binder and using different conforming pressures by application of loads ranging from 1 ton up to 5 tons in the press, which corresponds to pressures ranging from 74 up to 370 MPa. The obtained results show that 1 and 3 tons are appropriate to synthesize a proper monolith without any structural damage, either internally or externally (after visual inspection). Despite the structural strength of carbon network, loads around 3 tons constitute an upper limit.

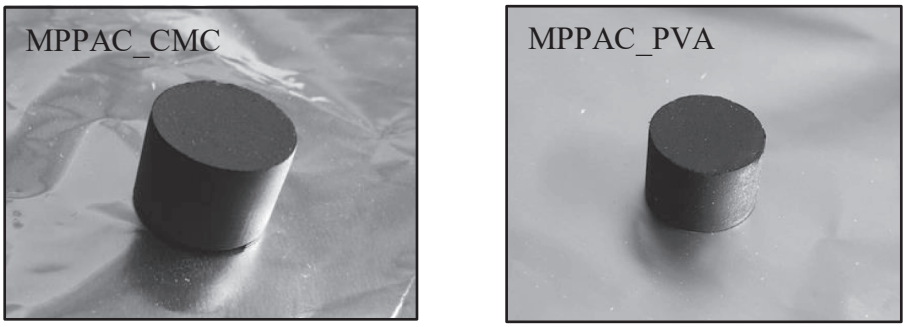

Fig. 3. Photographs of a typical carbon monolith synthesized using 5 wt% of carboxymethyl cellulose (CMC) or polyvinyl alcohol (PVA) as a binder (i.d. 1.3 cm; height ≈ 0.7–0.8 cm) and 74 MPa of conforming pressure.

Conforming loads above this threshold value (e.g., 5 tons) become detrimental with a significant decrease in the BET surface area and methane adsorption capacity.

Last but not least, the amount of binder incorporated was evaluated in terms of porous structure and mechanical properties of the final monolith and, in terms of adsorption performance for methane at 4.0 MPa and 298 K. At this point it is important to highlight that methane adsorption measurements were performed using the complete monoliths in a specially designed high-pressure cell, thus avoiding uncertainties when breaking the monoliths into small pieces. Nitrogen adsorption/desorption measurements at 77 K (Fig. 4) show that the incorporation of the binder becomes detrimental for the adsorption performance due to the partial blocking of the porosity. The BET surface area decreases from 2300 m^2/g in the original carbon down to 2000 m^2/g for the samples with 12 wt% CMC (Table S7). A similar scenario takes place for methane adsorption at 4.0 MPa, with a progressive decrease in the excess gravimetric storage capacity from 17.9 wt% down to 15 wt% (Table S8). Interestingly, the incorporation of the binder gives rise to a significant effect in the density of the final monolith with an upper limit of 0.47 g/cm^3 for monoliths with 12 wt% CMC. Despite the detrimental effect of the binder in the adsorption performance, the associated increase in the density allows to compensate, the volumetric adsorption capacity reaching an upper value of 104 V/V for the sample with 10 wt% CMC. The volumetric storage capacity achieved with the full monoliths (ca. 100–105 V/V) is lower than the best values reported in the literature for activated carbon-based monoliths (ca. 140–190 V/V) [14,37,50,51]. However, it is important to highlight that, contrary to some papers in the literature, i) the reported values in this study are excess adsorption capacities and not total storage capacities, ii) monoliths were not optimized (e.g., blending bimodal carbon powders), iii) considered densities are real volumetric mass densities and not estimated packing densities measured under pressure and iv) the methane capacity was measured using the complete monolith after the conforming step.

To end up, the mechanical properties of the synthesized monoliths with a different proportion of CMC have been tested using the compressive tests. Figure S5 and Table S8 show that the mechanical properties are rather similar for all monoliths evaluated, independently of the amount of binder incorporated. However, the compressive modulus and compressive strength at failure anticipate a certain improvement for sample MPPAC_8CMC, although small. In any case, Figure S5 suggest that 10 wt% can be anticipated as an upper limit for a proper mechanical performance, higher contents in CMC having a detrimental effect in the resistance of the monoliths to failure.

Overall, these results show that CMC in a percentage of 10 wt% and with a conforming pressure of 222 MPa (or a load of 3 tons) are proper experimental conditions to prepare carbon monoliths with an optimum porous structure and packing density to achieve an upper value in the methane volumetric adsorption capacity.

3.2.2. *Effect of the additives in the conformed monoliths*

In a final step, the best conditions identified in previous sections were applied to synthesized composite monoliths containing either graphene or graphite in their formulation, as described in section 3.1.2. Fig. 5 shows the nitrogen adsorption/desorption isotherms for the different monoliths conformed using CMC (10 wt%) and either pure carbon or carbon-based composites. As expected, the incorporation of the binder and the graphite/graphene in the composition gives rise to a progressive decrease in the textural parameters, preferentially a partial blocking of the narrow microporosity, and a decrease in the total adsorption capacity at $p/p_0 = 1$. This is clearly reflected in the nitrogen

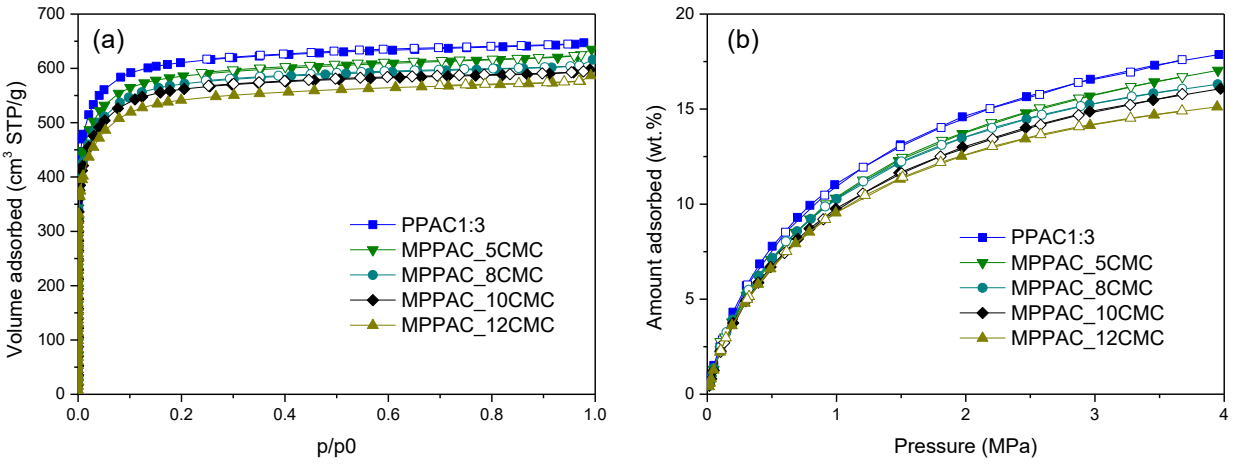

Fig. 4. (a) Nitrogen adsorption/desorption isotherms at 77 K for the PPAC1:3 samples after a conforming step using different concentrations of CMC (5–12 wt%); (b) Excess methane adsorbed at 298 K and up to 4.0 MPa.

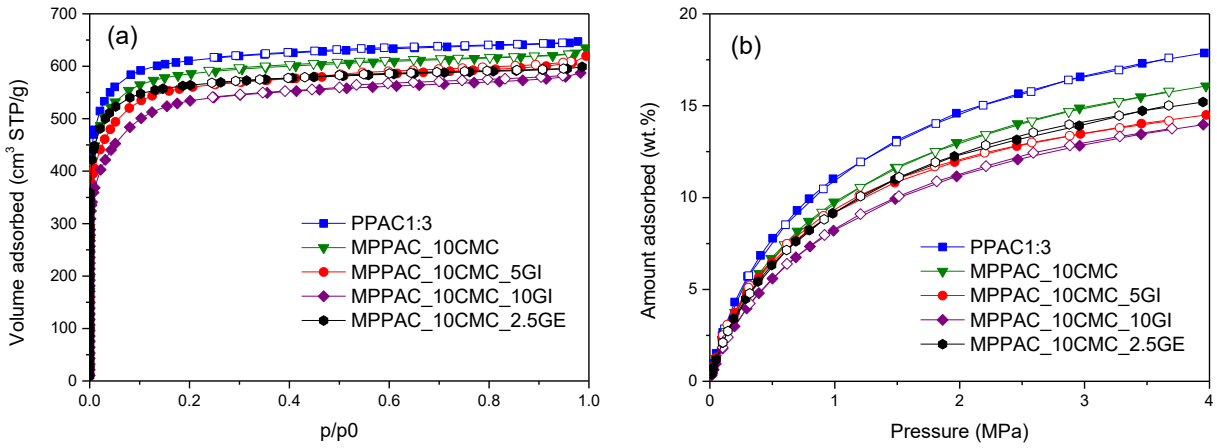

Fig. 5. (a) Nitrogen adsorption/desorption isotherms at 77 K for the PPAC1:3 samples after a conforming step using 10 wt% CMC and after incorporation of either graphite or graphene as additives; (b) Excess methane adsorbed at 298 K and up to 4.0 MPa for these samples.

isotherms with a broadening of the knee at low relative pressures in the final monolith. BET surface area decreases from 2300 m^2/g in the original carbon PPAC1:3 down to ca. 2000–2100 m^2/g, after the incorporation of the binder, the corresponding additive and the application of a conforming step. The reduction in the textural characteristics of the final composite is understandable due to the non-porous nature of the binder and the additives incorporated (although some contribution from the additives after the KOH activation treatment cannot be ruled out). Consequently, binder and additives contribute to the weight but not to the porous structure of the final monolith, thus explaining the much lower surface area for sample MPPAC_10CMC_10GI (i.e. 10 wt% binder and 10 wt% graphite).

A similar scenario takes place for the methane adsorption measurements at 298 K and 4.0 MPa. Incorporation of binder and additives gives rise to a decrease in the methane storage capacity, the decrease being proportional to the amount of additive incorporated, i.e. MPPAC_10CMC > MPPAC_10CMC_2.5GE > MPPAC_10CMC_5GI > MPPAC_10CMC_10GI. The excess methane adsorbed (gravimetrically) decreases from 17.9 wt% in the original powder sample to 16.1 wt% after a conforming step with CMC and down to 13–15 wt% after the incorporation of graphite or graphene additives (Table S10). These results clearly show that the incorporation of additives becomes detrimental to the adsorption performance of the monoliths. However, the partial clogging of the 3D porous network is accompanied by a significant increase in the density of the final monolith, from 0.38 g/cm^3 in the original compacted powder up to 0.52 g/cm^3 in the monolith with 10 wt % graphite. Interestingly, the increase in the final density of the monolith is sufficient to compensate the decrease in the excess gravimetric capacity so that the volumetric capacity of the monoliths for methane storage (V/V) is always above 100 V/V, independently of the additive incorporated. As described in the introduction, the main role of the additives is to incorporate new properties in the monolith without compromising the adsorption properties. To this end, the thermal and mechanical properties of the monoliths have been tested and compared to the MPPAC_10CMC sample without additives.

Fig. 6 and Table S10 show that the incorporation of graphite in the formulation of the MPPAC_10CMC monolith gives rise to a tremendous increase in the mechanical properties, with close to a twofold increase in the compressive modulus and compressive strength at failure for the monolith with 10 wt% graphite. Concerning the thermal properties,

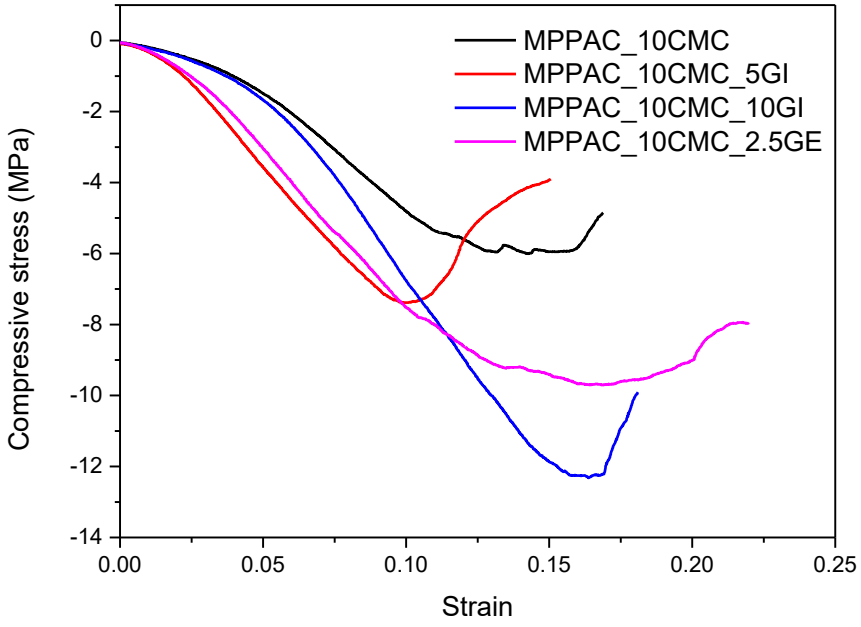

Fig. 6. Compressive stress–strain curves for the MPPAC monoliths prepared with 10 wt% CMC and modified with either graphite or graphene.

Table S10 shows that the incorporation of graphite is able to increase 19 % and 50 % the thermal conductivity of the original unmodified monolith, for samples with 5 wt% and 10 wt% graphite, respectively. These results are highly encouraging since incorporation of only 10 wt% of graphite allows to infer a 105 % increase in the compressive strength and 50 % increase in the thermal conductivity.

At this point it is important to highlight the effect of graphene. Incorporation of a small amount of graphene (2.5 wt%) in the final formulation is sufficient to increase the mechanical and thermal properties of the monoliths highly above the values achieved with the monolith with 5 wt% graphite, i.e. the graphene-based monolith exhibits a surprisingly large stability towards failure, and a thermal conductivity comparable to the one of the monolith with 10 wt% graphite. Overall, these results demonstrate the beneficial effect of these additives to increase the mechanical and thermal properties of activated carbon monoliths, preferentially when using graphene as an additive without compromising their adsorption properties at high pressures.

4. Conclusions

A series of activated carbon materials have been prepared from petroleum pitch residues using KOH as activating agent. Nitrogen adsorption measurements show that the synthesized samples exhibit a highly developed porous structure (up to 3300 m^2/g), and a high methane adsorption capacity (up to 20 wt% at 4 MPa and 298 K). These carbon materials have been modified through the incorporation of carbon-based additives with high thermal conductivity (graphite or graphene). The incorporation of the additives in the initial stages of the synthesis process allows to design composites with improved packing density without compromising the adsorption performance of the parent carbon. These powder samples can be easily conformed into monoliths after the incorporation of a proper amount of binder. Experimental results show that carboxymethyl cellulose in a proportion of 10 wt% allows to obtain carbon monoliths with very promising mechanical properties (compressive strength at failure up to 6 MPa). Incorporation of graphite or graphene in the formulation of these monoliths allows to increase up to twofold the compressive strength and up to 50 % the thermal properties, without compromising the volumetric adsorption capacity.

CRediT authorship contribution statement

S. Reljic: Investigation, Data curation, Formal analysis. **C. Cuadrado-Collados:** Investigation, Data curation, Formal analysis. **J. Farrando-Perez:** Investigation, Data curation, Formal analysis. **E.O. Jardim:** Conceptualization, Methodology. **M. Martinez-Escandell:** Conceptualization. **J. Silvestre-Albero:** Writing – review & editing.

Declaration of competing interest

The authors declare that they have no known competing financial interest or personal relationships that could have appeared to influence the work reported in this paper.

Acknowledgement

Authors would like to acknowledge financial support from the Ministerio de Ciencia e Innovación (Project PID2019-108453GB-C21), MCIN/AEI/10.13039/501100011033 and EU "NextGeneration/PRTR (Project PCI2020-111968 /3D-Photocat) and NATO SPS program (Project G5683).

Appendix A. Supplementary data

Supplementary data to this article can be found online at https://doi.org/10.1016/j.fuel.2022.124753.

References

[1] Li H, Wang K, Sun Y, Lollar CT, Li J, Zhou H-C. Recent advances in gas storage and separation using metal-organic frameworks. Mater Today 2018;21:108–21.
[2] Hiraide S, Sakanaka Y, Kajiro H, Kawaguchi S, Miyahara MT, Tanaka H. High-throughput gas separation by flexible metal-organic frameworks with fast gating and thermal management capabilities. Nature Commun 2020;11:3867.
[3] Morris JR, Contescu CI, Chisholm MF, Cooper VR, Guo J, He L, et al. Modern approaches to studying gas adsorption in nanoporous carbons. J Mater Chem A 2013;1:9341–50.
[4] Choi P-S, Jeong J-M, Choi Y-K, Kim M-S, Shin G-J, Park S-J. A review: methane capture by nanoporous carbon materials for automobiles. Carbon Letters 2016;17:18–28.
[5] Policicchio A, Filosa R, Abate S, Desiderio G, Colavita E. Activated carbon and metal-organic framework as adsorbent for low-pressure methane storage applications: an overview. J Porous Mater 2017;24:905–22.
[6] Travlou NA, Seredych M, Rodríguez-Castellón E, Bandosz TJ. Activated carbon-based gas sensors: effects of surface features on the sensing mechanism. J Mater Chem A 2015;3:3821–31.
[7] Small LJ, Schindelholz ME, Nenoff TM. Hold on tight: MOF-based irreversible gas sensors. Ind Eng Chem Res 2021;60:7998–8006.
[8] He S, Wu L, Li X, Sun H, Xiong T, Liu J, et al. Metal-organic frameworks for advanced drug delivery. Acta Pharm Sinica B 2021;11:2362–95.
[9] Sun Y, Zheng L, Yang Y, Qian X, Fu T, Li X, et al. Metal-organic framework nanocarriers for drug delivery in biomedical applications. Nano-micro Lett 2020;12:103.
[10] Wang L, Zheng M, Xie Z. Nanoscale metal-organic frameworks for drug delivery: a conventional platform with new promise. J Mater Chem B 2018;6:707–17.
[11] Gandara-Loe J, Ortuño-Lizarán I, Fernández-Sanchez L, Alió JL, Cuenca N, Vega-Estrada A, et al. Metal-organic frameworks as drug delivery platforms for ocular therapeutics. ACS Appl Mater Interf 2019;11:1924–31.
[12] Crittenden B, Patton A, Jouin C, Perera S, Tennison S, Botas Echevarria JA. Carbon monoliths: A comparison with granular materials. Adsorption 2005;11:537–41.
[13] Wang F, Liu J, Zeng H. Interactions of particulate matter and pulmonary surfactant: Implications for human health. Adv Colloid Interface Sci 2020;284:102244.
[14] Lozano-Castelló D, Cazorla-Amorós D, Linares-Solano A, Quinn DF. Activated carbon monoliths for methane storage: influence of binder. Carbon 2002;40:2817–25.
[15] Ubago-Perez R, Carrasco-Marin F, Fairen-Jimenez D, Moreno-Castilla C. Granular and monolithic activated carbons from KOH-activation of olive stones. Microp Mesop Mater 2006;92:64–70.
[16] Lu A-H, Smatt J-H, Backlund S, Linden M. Easy and flexible preparation of nanocasted carbon monoliths exhibiting a multimodal hierarchical porosity. Microp Mesop Mater 2004;72:59–65.
[17] Oschatz M, Borchardt L, Senkovska I, Klein N, Leistner M, Kaskel S. Carbon dioxide activated carbide-derived carbon monoliths as high performance adsorbents. Carbon 2013;56:139–45.
[18] Djeridi W, Ouederni A, Wiersum AD, Llewellyn PL, El Mir L. High pressure methane adsorption on microporous carbon monoliths prepared by olive stones. Mater Lett 2013;99:184–7.
[19] Tian T, Zeng Z, Vulpe D, Casco ME, Diviniti G, Midgley PA, et al. A sol-gel monolithic metal-organic framework with enhanced methane uptake. Nat Mater 2018;17:174–9.
[20] Connolly BM, Aragones-Anglada M, Gandara-Loe J, Danaf NA, Lamb DC, Mehta JP, et al. Tuning porosity in macroscopic monolithic metal-organic frameworks for exceptional natural gas storage. Nature Commun 2019;10:2345.
[21] Policicchio A, Maccallini E, Agostino RG, Ciuchi F, Aloise A, Giordano G. Higher methane storage at low pressure and room temperature in new easily scalable large-scale production activated carbon for static and vehicular applications. Fuel 2013;104:813–21.
[22] Inomata K, Kanazawa K, Urabe Y, Hosono H, Araki T. Natural gas storage in activated carbon pellets without a binder. Carbon 2002;40(1):87–93.
[23] Liu C-F, Liu Y-C, Yi T-Y, Hu C-C. Carbon materials for high-voltage supercapacitors. Carbon 2019;145:529–48.
[24] Wang J, Zhang X, Li Z, Ma Y, Ma L. Recent progress of biomass-derived carbon materials for supercapacitors. J Power Sources 2020;451:227794.
[25] Lamari M, Aoufi A, Malbrunot P. Thermal effects in dynamic storage of hydrogen by adsorption. AIChE J 2000;46:632–46.
[26] Hao J, Liang B, Sun W. Experimental study on the thermal effect during gas adsorption and desorption on the coal surface. ACS Omega 2021;6:1603–11.
[27] Sakanaka Y, Hiraide S, Tanaka H, Hiratsuka T, Kojima N, Yamane Y, et al. Efficiency of thermal management using phase-change material for nonisothermal adsorption process. Ind Eng Chem Res 2020;59:14485–95.
[28] Strizhenov EM, Chugaev SS, Meńshchikov IE, Shkolin AV, Zherdev AA. Heat and mass transfer in an adsorbed natural gas storage system filled with monolithic carbon adsorbent during circulating gas charging. Nanomaterials 2021;11:3274.
[29] Corgnale C, Hardy B, Chahine R, Zacharia R, Cossement D. Hydrogen storage in a two-liter adsorbent prototype tank for fuel cell driven vehicles. Appl Energy 2019;250:333–43.
[30] Qingrong Z, Weidong Z, Xuan Z, Mengbo W, Shengping L. Evaluation of the effects of heat conducting enhancement measurements on MOFs hydrogen storage system for ships propulsion plant. Intern J Hydrogen Energy 2021;46:18412–22.
[31] Zhang Y, Fan W, Huang Y, Zhang C, Liu T. Graphene/carbon aerogels derived from graphene crosslinked polyimide as electrode materials for supercapacitors. RSC Adv 2015;5:1301–8.

[32] Menard D, Py X, Mazet N. Activated carbon monolith of high thermal conductivity for adsorption processes improvement: Part A: Adsorption step. Chem Eng Processing: Process Intens 2005;44:1029–38.
[33] Kuwagaki H, Meguro T, Tatami J, Komeya K, Tamura K. An improvement of thermal conduction of activated carbon by adding graphite. J Mater Sci 2003;38:3279–84.
[34] Yu Y, Du J, Liu L, Wang G, Zhang H, Chen A. Hierarchical porous nitrogen-doped partial graphitized carbon monoliths for supercapacitors. J Nanopart Res 2017;19:119.
[35] Sevilla M, Fuertes AB. Fabrication of porous carbon monoliths with a graphitic framework. Carbon 2013;56:155–66.
[36] Nguyen HGT, et al. A reference high-pressure CH4 isotherm for zeolite Y: results of an interlaboratory study. Adsorption 2020;26:1253–66.
[37] Wang J, Kaskel S. KOH activation of carbon-based materials for energy storage. J Mater Chem 2012;22:23710–25.
[38] Lillo-Rodenas MA, Cazorla-Amorós D, Linares-Solano A. Understanding chemical reactions between carbons and NaOH and KOH: An insight into the chemical activation mechanism. Carbon 2003;41:267–75.
[39] Sevilla M, Valle-Vigon P, Fuertes AB. N-doped polypyrrole-based porous carbons for CO2 capture. Adv Funct Mater 2011;21:2781–7.
[40] Casco ME, Martinez-Escandell M, Gadea-Ramos E, Kaneko K, Silvestre-Albero J, Rodríguez-Reinoso F. High-pressure methane storage in porous materials: Are carbon materials in the pole position? Chem Mater 2015;27:959–64.
[41] Rodriguez-Reinoso F, Silvestre-Albero J. Methane storage on nanoporous carbons. In: Kaneko K, Rodriguez-Reinoso F, editors. Nanoporous materials for gas storage. Springer; 2019. p. 209–26.
[42] Balderas-Xicohtencatl R, Schlichtenmayer M, Hirscher M. Volumetric hydrogen storage capacity in metal-organic frameworks. Energy Technol 2018;6:578–82.
[43] Cacciola G, Restuccia G, Mercadante L. Composites of activated carbon for refrigeration adsorption machines. Carbon 1995;33:1205–10.
[44] Griesinger A, Spindler K, Hahne E. Measurements and theoretical modelling of the effective thermal conductivity of zeolites. Int J Heat and Mass Transfer 1999;42:4363–74.
[45] Huang BL, Ni Z, Millward A, McGaughey AJH, Uher C, Kaviany M, et al. Thermal conductivity of metal-organic framework (MOF-5): Part II. Measurements. Int J Heat and Mass Transfer 2007;50:405–11.
[46] Peng Y, Krungleviciute V, Eryazici I, Hupp JT, Farha OK, Yildirim T. Methane storage in metal-organic frameworks: Current records, surprise findings, and challenges. J Am Chem Soc 2013;135:11887–94.
[47] Wu X, Liu Y, Fang M, Mei L, Luo B. Preparation and characterization of carbon foams derived from aluminosilicate and phenolic resin. Carbon 2011;49:1782–6.
[48] Narasimman R, Prabhakaran K. Preparation of carbon foams by thermo-foaming of activated carbon powder dispersions in an aqueous sucrose resin. Carbon 2012;50:5583–93.
[49] Liu H, Li T, Huang T, Zhao X. Effect of multi-walled carbon nanotube additive on the microstructure and properties of pitch-derived carbon foams. J Mater Sci 2015;50:7583–90.
[50] Bose TK, Chahine R, St-Arnaud JM, **High-density adsorbent and method of producing same**, U.S. Pantent No. 4999330A, March 12, 1991.
[51] Celzard A, Fierro V. Preparing a suitable material designed for methane storage: A comprehensive report. Energy Fuels 2005;19:573–83.